

An Aquatic Image Compression Scheme based on Optimized Deep Convolutional Autoencoder

Raj Kumar Paul*, Ankit Vishwakarma, Saravanan Chandran

Abstract— Nowadays, in daily life, several online platforms have generated an enormous amount of data, mainly images, audio, and video. Uncompressed multimedia information, such as images, graphics, audio, animation, and video, needs massive storage space and transmission bandwidth. Suitable image compression methods to overcome excessive data traffic are necessary. The image compression scheme reduces image size, which is beneficial for storage and transmission. Multiple techniques have been utilized to solve the difficulties, but most suffer a significant drawback: important information must be recovered in the reconstructed image. An optimized deep convolutional autoencoder model has been implemented using the deep learning approach for solving the challenges. The proposed model has many layers and filters to develop an effective, efficient image compression method. The unsupervised machine learning approach compresses the image using the backpropagation technique and finally reconstructs the image with minimum information loss. One new instance has been incorporated into the architecture to improve image compression performance. The methodology performed better at the time of image compression. Due to this problem, we select convolutional neural networks, followed by generative adversarial networks, as a solution to reduce diverse compression artifacts. This research covers the compression of underwater images based on a deep convolutional autoencoder. The concept of underwater image acquisition techniques and their analysis are also discussed. The proposed image compression approach is studied using performance parameters, like Space Saving (SS(%)), and PSNR is differentiated with state-of-the-art methods. Experimental outcomes indicate the proposed technique acquires higher SS (%) and PSNR, reduced space complexity, and better image quality than the existing image compression system. Using the Marine Animals dataset, the proposed model achieved SS (%) 83.33, PSNR 72.60 (dB), and Structural Similarity Index Measurement (SSIM) 0.9517 values. Also, the proposed model achieved SS (%) 83.33, PSNR 74.77 (dB), and SSIM 0.9766 values using the Sea Animal dataset. However, it has produced a new root in the future investigation for the improvement of the method, such as better performance factor of compression and minimization of data loss for the 3D image.

Index Terms—Convolutional Neural Networks, Compression Ratio, Convolutional Autoencoder, Peak Signal to Noise Ratio, Space Saving SS(%), Structural Similarity Index Measurement (SSIM)

I. INTRODUCTION

IMAGE compression underwater images are applied in many systems, such as underwater robotics, autonomous underwater vehicles, marine research, etc. [1], [2], [22], [23].

Manuscript received May 02, 2023; revised Nov 21, 2023.

Raj Kumar Paul is a Ph.D. research scholar of the NIT, Durgapur, India (corresponding author to provide e-mail: rajkumar.rkp@gmail.com).

Ankit Vishwakarma is a graduate student of National Institute of Technology, Durgapur, India. (e-mail: av.19u10072@btech.nitdgp.ac.in).

Saravanan Chandran is an Associate Professor of National Institute of Technology, Durgapur, India. (e-mail: cs@cse.nitdgp.ac.in).

An image is a record of visual perception. Nowadays, images are essential information; it needs to be compressed to work in applications like underwater image [5], [7], [8], [31]. The requirement of compression depends on the objective of the application. The image coding method is significant for image transmission and storage due to storage and transmission bandwidth limitations. Image compression aims to define the image that requires the minimum bits without losing the vital information of the input image. The compression approach is rapidly developed for large image datasets such as aquatic, multimedia, medical, and satellite images. With the improvement of methodology, a massive amount of image datasets is transmitted and stored correctly using efficient image compression techniques [7]-[9]. Different algorithms perform compression differently, namely lossless, and lossy. Lossless schemes retain the same information as the input image, and if some information is lost, it is called a lossy image compression technique [18]-[20]. Some compression techniques are designed for specific images; it is not suitable for other images. A few algorithms change a few parameters to enhance the compression performance of the image. Data encoding is a superset of image encoding that encodes the original image with minimum bits [1]. The image compression aim is to minimize the image content's redundancy and improve the efficiency of storing or transmitting images [14], [16], [18]-[20].

Compression ratio (CR) is a ratio of AI and CI, where AI is the actual image, and CI is the compressed image [18]-[20]. Image compression is a process of a compact image representation to reduce the image size for storage and transmission requirements. It defines the problem of minimizing the amount of information required to construct a digital image with quality. All the images have redundant information. Redundancy means duplicate information present in the image. It is repeating pixel values or pixel value patterns in the original image. The compression process takes advantage of the redundant pixel value of the original image. The redundancy reduction process achieves the storage size saving of an input image. Image compression is achieved when one or more redundancies are present in the image. There are three essential data redundancy techniques in image compression. Compression is achieved by removing one or more primary data redundancies [13], [20], [33].

- Image compression provides cost savings for sending an image over the communication network where the transmission cost is based on time.
- Image compression reduces storage requirements.
- Image compression reduces overall execution time.
- Image compression reduces transmission errors because fewer bits are transferred [18] - [20].
- Image compression protects against unlawful monitoring.

The remaining sections of the article are: Section 2 defines some previous research, Section 3 explains the proposed model description, Section 4 describes the experiment process, result, and analysis, and Section 5 concludes with references.

II. PREVIOUS RESEARCH WORKS

Various neural networks, as well as deep learning approaches, have been utilized for image compression. However, there were no efficient deep-learning algorithms. Toderici et al. developed one of the most successful deep-learning approaches. Recurrent neural network (RNN) architecture performed slightly better than JPEG [15]. The JPEG compression method compressed a small amount of images for small images. This network follows the three stages of compression: encoding, quantization, and decoding. Encoding and decoding are done iteratively using two different architectures of RNNs [15], convolutional or deconvolutional (Long Short-Term Memory (LSTM)) and LSTMs. The advantage of this method was the higher compression ratio, while the disadvantage was that the procedure was time-consuming. The researcher recently implemented a compression network using GANs, achieving high-quality images at high compression rates. However, the reconstructed images differ slightly from the original [3], [7].

Internet-of-Things (IoT) has expanded to a new version, the Internet of Underwater Things (IoUT), which works underwater. IoUT applications include underwater environment surveillance systems, habitat observation of underwater animals, defense systems, and underwater disaster prediction processes. Transmission of images captured by intelligent underwater things was complicated due to the aquatic atmosphere and necessary image transmission approach in the IoUT. The image compression model was implemented based on discrete wavelet transform (DWT) and deep learning in IoUT. A convolution neural network (CNN) was used for compression and decompression to achieve a better compression model. The DWT-CNN model was superior to super-resolution CNN (SR-CNN), JPEG, and JPEG2000 as per the performance and quality of the reconstructed image. The DWT-CNN procedure achieved PSNR value and space-saving (SS%) [2].

The image plays a more significant role than the text and audio files in underwater data storage and transmission. However, a lower transmission rate is due to the limited bandwidth of aquatic image communication, which only affords a limited image. Before transmission, image compression is an essential approach in underwater transmission [24]. The compression techniques are applied to the underwater image. The underwater image has multiple degradations from the natural image due to the optical transmission features. Shallow underwater illumination causes more blurring and fading than the air environment. It is challenging to reduce the bitrate of the compressed underwater image while the compressed image quality remains unchanged. The research considered the Human Visual System (HVS) during underwater image communication's compressing and evaluating stages. The author developed a methodology for underwater image compression. Following the HVS, the chrominance perception operator was initially implemented in research to

avoid the invisible chrominance shift, which was broadly excited in underwater imaging to enhance the image compression ratio. After that, the underwater image's depth of field was usually shallow, and most usable images were targeted. The region of interest extraction approach uses a boolean map detection technique for compression to reduce the compression bitrate of the compressed underwater image. The degradation in some regions of the image is due to the grainy underwater image having low contrast. Also, the image processing field used a difference sensing method using the spatial and frequency domain masking properties of HVS. Above, three characteristics were combined; the hybrid wavelet approach and asymmetric coding technique were used to improve the compression model for underwater images, achieving better-reconstructed image quality and minimizing redundancy [1]. The experimental outcomes showed that the model was useful for the implicit image features and maximized the redundancy of images without losing the information of the original underwater image that is reconstructed image quality.

III. PROPOSED MODEL

The section presents the multiple steps of compression based on Convolutional Neural Networks (CNNs), which have many layers, namely Convolution, Max pooling, and Fully Connected Layer. Also, the section presents the proposed image compression model based on an optimized deep convolutional autoencoder approach.

A. Convolutional Neural Networks

An artificial Neural Network (ANN) is a computational processing system to compute complex problems motivated by human nervous systems (HNS). The primary element of HNS is neurons, also known as nodes in the ANNs. ANNs have many interconnected computational nodes that perform operations jointly and follow the distributed pattern to collectively compute from the input layer to optimize its final output layer. Fig. 1 presents the fundamental concept of CNNs, and Fig. 2 shows the basic architecture of CNNs. The neural networks model loads the input as a multidimensional vector to the input layer after that, distributes it to the hidden layers (HL). The HL creates decisions from the previous layer's output and weighs how a stochastic modification within it, called the learning process, deteriorates, or enhances the outcome.

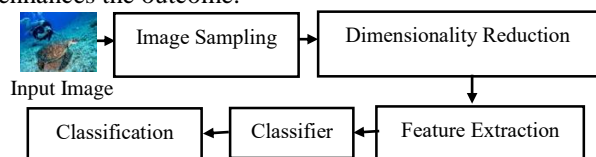


Fig. 1. Basic Concept of Convolutional Neural Networks (CNNs)

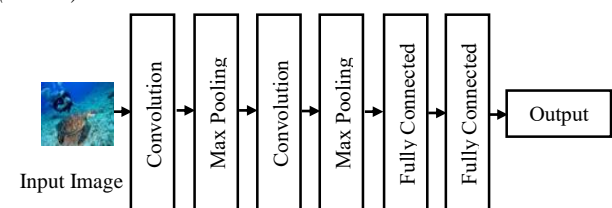


Fig. 2. Basic Architecture of Convolutional Neural Networks (CNNs)

Deep learning has many HL that connect one after another as a stack. The CNNs are like ANNs because both approaches contain self-optimized neurons based on the learning process. Each neuron takes input and operates like a scalar product using a non-linear operation in the ANNs. From the input original image vectors to the outcome of the class score, the whole network expresses a reactive score function: the weight (W). The rearmost layer consists of loss functions connected with the classes and the rules and regulations implemented for basic ANNs. The CNNs are applied in pattern recognition based on image datasets, and ANNs are the superset of CNNs [34] - [37]. CNN encodes images based on specific network architecture features, creating a network more suitable for image compression as a concentrated task while minimizing the parameters needed to construct the network's model [4], [25] - [29].

B. Convolutional Autoencoder (CAE)

Autoencoder is a deep learning approach for transforming image data from higher to lower dimensions. It encodes the data, whatever its size, into a one-dimensional vector, which decodes to reconstruct the original image. The autoencoder generates original images [6] – [8], [31]. Fig. 3 shows a compression and decompression model diagram based on the optimized deep convolutional autoencoder.

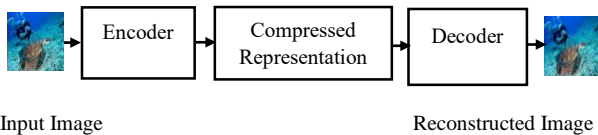


Fig. 3. Diagram of Compression and Decompression model Convolutional Autoencoder

The encoder takes the original image as input with two or more dimensions and generates a single one-dimension vector representing the image. The element's number varies depending on the problem in the one-dimension vector. It has one or more features, some elements in the vector, and more complexity in reconstructing the input image correctly. The model compresses the image by analyzing the original image in a vector of relatively few elements. The decoder reconstructs the image with higher quality. The decoder is the vice versa process of the encoder [10] – [12], [30].

C. Models Description

This subsection presents the proposed compression model. Fig. 4 has been described the flow diagram of the proposed compression method (ESDCA-DSDCA). The image compression model has two procedures: the encoding model is the encoder, and the decoding model is the decoder. The encoding model takes an image as the input to the input layer, and then the convolution technique Conv2D-1 has convolution operation with stride two and activation function Relu. The convolution technique Conv2D-2 has convolution operation with stride two and activation function Relu. The convolution technique Conv2D-3 has convolution operation with stride two and activation function Relu. Finally, the output layer has generated a compressed representation. The decoding model started with compressed representation as the input layer. Then, the convolution technique De-Conv2D-1 has convolution operation with stride two and activation

function Relu. The convolution technique De-Conv2D-2 has convolution operation with stride two and activation function Relu. The convolution technique De-Conv2D-3 has convolution operation with stride two and activation function Sigmoid. Then, the output layer generated a reconstructed Image. Finally, the decoder model has computed the CR, SS (%), MSE, and PSNR. The ESDCA-DSDCA model's output and the existing model's output have been compared with performance measurements like SS (%) and visual quality measurements PSNR. Algorithm1 presents the Encoding Scheme based on the Deep Convolutional Autoencoder model, which is ESDCA. Algorithm2 describes the Decoding Scheme based on the Deep Convolutional Autoencoder model, ESDCA.

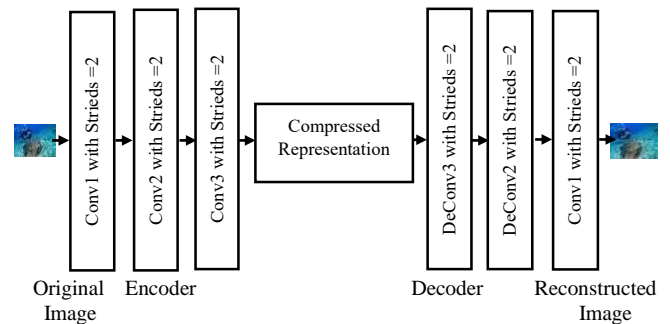


Fig. 4. The proposed model diagram (ESDCA-DSDCA)

Algorithm 1: Encoding Scheme based on Deep Convolutional Autoencoder (ESDCA)

Input: Original Images (Input from the dataset).

Output: Compressed Images

1: $(OI_{u,v}) \leftarrow$ Original Image

2: Input Layer

3: Conv2D,

Activation = relu,

Padding = Same,

Strieds = 2

4: Conv2D,

Activation = relu,

Padding = Same,

Strieds = 2

5: Conv2D,

Activation = relu,

Padding = Same,

Strieds = 2

7: Output Layer

8: *Compressed Images* $\leftarrow (CI_{u,v})$

Algorithm 2: Decoding Scheme based on Deep Convolutional Autoencoder (DSDCA)

Input: Compressed Images

Output: Original Image

1: $(CI_{u,v}) \leftarrow$ Compressed Images

2: Input Layer

3: De-Conv2D,

Strieds = 2

Activation = relu,

Padding = Same,

4: De-Conv2D,

Strieds = 2

- Activation = *relu*,
- Padding = *Same*,
- 5: *De-Conv2D*,
- Activation = *Sigmoid*
- Padding = *Same*,
- 6: *Output Layer*
- 7: *Reconstructed Image* $\leftarrow (RI_{u,v})$
- 8: *Calculate the CR, MSE, and PSNR values*

IV. EXPERIMENTS AND OUTCOME ANALYSIS

This section represents the experimental setup and outcome analysis of the ESDCA-DSDCA model. The experiment was performed on the Python platform. Fig. 5 and Fig. 6 show the sample 30 images of the datasets, namely the underwater Image Datasets- Marine Animals and Sea Animal [22], [17]. The proposed Optimized Deep Convolutional Autoencoder model-based approach is implemented in Python 3.11.1. using the Numpy 1.25.1 and Scikit-learn 1.0.1. We have compressed all images of the underwater Image Dataset using the ESDCA-DSDCA models.

A. Datasets: Underwater Image Datasets

Maximum life forms began their evolution in aquatic environments. The oceans provide about 90% of the world's living space in terms of volume. Fish, which are only found in water, is the first known vertebrates. Some of these transformed into amphibians, which dwell on land and water for parts of the day. A few subgroups of one group of amphibians, which also included sea turtles, seals, manatees, and whales, developed into reptiles and mammals. Fig. 5 shows the uncompressed training dataset's standard input images that test the dataset.

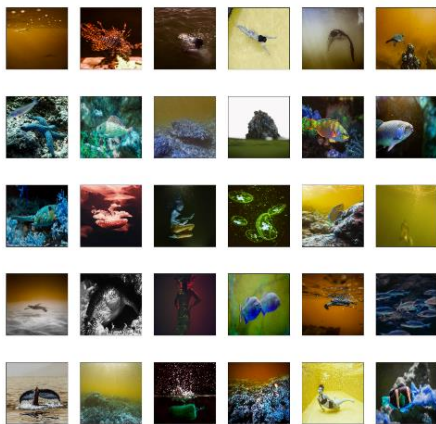


Fig. 5. The standard input images: Uncompressed Training Dataset: Marine Animals

Some underwater habitats, such as kelp and other algae, are supported by plant life that grows in the water. The base of the ocean food chain is made up primarily of phytoplankton, an essential primary producer. The dataset contains 2587 images of marine animals [22]. There are 19 classes; the training images are 90%, and the test images are 10%. Fig. 7 shows the standard input images, test dataset: uncompressed test dataset. The size of the images is 128x128x3. The model has achieved the optimum outcome after 25 epochs. Also, the Sea Animal Data Set contains 13082 [17]. There are 19 classes; the training images are 90%, and the test images are 10%. Fig. 6 shows the uncompressed training dataset's

standard input images that test the dataset. Fig. 8 shows the familiar input images, test dataset: uncompressed test dataset. The image size is 128x128x3. The model has achieved the optimum outcome after 25 epochs.



Fig. 6. The standard input images: Uncompressed Training Dataset: Sea Animal

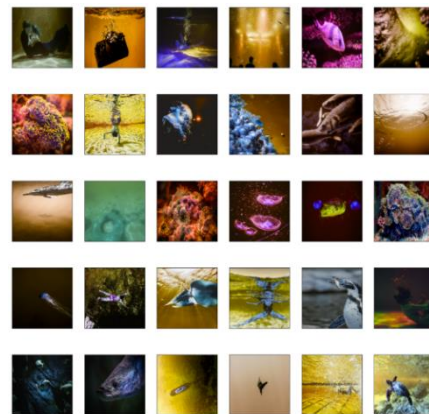


Fig. 7. The standard input images: Uncompressed Test Dataset: Marine Animals

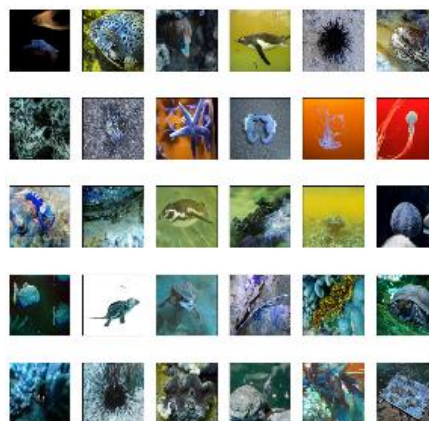


Fig. 8. The standard input images: Uncompressed Test Dataset: Sea Animal

B. Performance Parameters

This section uses four parameters to measure the performance of the ESDCA-DSDCA image coding scheme.

Space Saving (SS (%)): CR is the ratio between the size of the original image (OI) and the size of the compressed image (CI). Eq. (1) defines the calculation formula for the CR value of the ESDCA-DSDCA models. SS (%) measures the

compression of the OI based on the CI. We have used the CR value to calculate the percentage of savings for storage requirement, that is, the SS (%) value for the ESDCA-DSDCA models [2, 21].

$$CR = \frac{OI}{CI} \quad (1)$$

Peak Signal to Noise Ratio (PSNR): Mean Square Error (MSE) shows the error in the output image CI(m,n) compared with the input image OI(m,n) to examine the quality of the CI(m,n). MSE measures the distortion of the reconstructed image of the ESDCA-DSDCA model. A defines the rows, and B represents the columns of CI and OI images. Eq. (2) denotes the formula used to calculate the MSE value of the ESDCA-DSDCA models. It is used to analyze the ESDCA-DSDCA model based on image quality compression. PSNR computes the total noises in the image. R is the maximum pixel value in the image matrix. Eq. (3) defines the formula used to determine the PSNR value of the ESDCA-DSDCA models [2, 21].

$$MSE = \frac{1}{A*B} \sum_{l=1}^A \sum_{j=1}^B (OI(m,n) - CI(m,n))^2 \quad (2)$$

$$PSNR = 10 * \log_{10} * \frac{R^2}{MSE} \text{ (dB)} \quad (3)$$

Structural Similarity Index Measurement (SSIM): is the image quality measurement matrix [21]. The input image and the reconstructed image are compared and the structural similarity index value for image I₁ using I₀. where C₁ and C₂ are constant and equal to unity, and σ_x, σ_y, μ_x, μ_y and σ_{xy} are the standard deviations, local means, and cross co-variances for the images I₁, I₀, define as Eq. (4), formula used to determine the SSIM value of the ESDCA-DSDCA models.

$$SSIM(I_1, I_0) = \frac{(2\mu_x\mu_y + C_1)(2\sigma_{xy} + C_2)}{(\mu_{2x} + \mu_{2y} + 1)(\sigma_{2x} + \sigma_{2y} + C_2)} \quad (4)$$

C. Experimental Results Interpretation

The contents of Table I and Table II have illustrated the ESDCA-DSDCA model's experimental results. Fig. 9 show the reconstructed images of the ESDCA-DSDCA model.

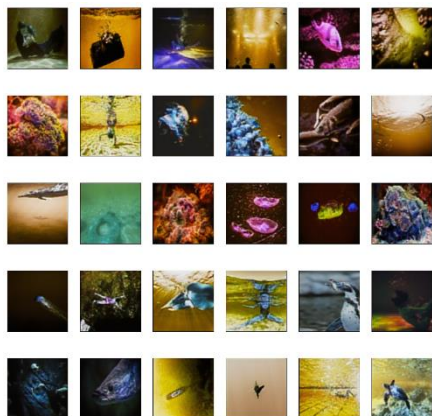


Fig. 9. Experimental Results: Reconstructed Image Data Set: Marine Animals

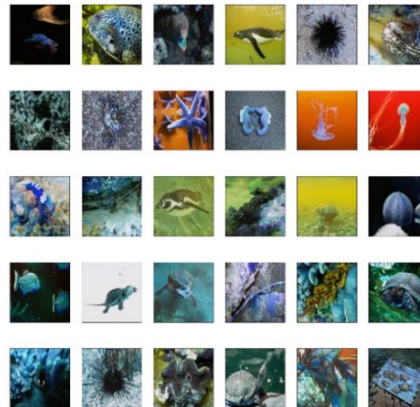


Fig. 10. Experimental Results: Reconstructed Image Data Set: Sea Animal

TABLE I
EXPERIMENTAL RESULTS OF ESDCA-DSDCA
FOR DATA SET: MARINE ANIMALS

Sl. No.	Test Images	CR	MSE	PSNR (dB)	SSIM
1.	Image-1	5.81	0.001157	77.49	0.9642
2.	Image-2	6.01	0.006046	70.31	0.9379
3.	Image-3	6.00	0.002003	75.11	0.9257
4.	Image-4	6.30	0.001742	75.71	0.9337
5.	Image-5	6.01	0.005437	70.77	0.9257
6.	Image-6	6.00	0.004289	71.80	0.9396
7.	Image-7	6.01	0.012967	67.00	0.9402
8.	Image-8	5.90	0.017304	65.74	0.9793
9.	Image-9	6.01	0.003072	73.25	0.9322
10.	Image-10	6.01	0.008334	68.92	0.9696
11.	Image-11	6.00	0.002694	73.82	0.9921
12.	Image-12	5.90	0.002782	73.68	0.9702
13.	Image-13	6.01	0.001614	76.04	0.9527
14.	Image-14	6.00	0.000850	78.83	0.9733
15.	Image-15	6.10	0.010806	67.79	0.9368
16.	Image-16	6.01	0.007884	69.16	0.9418
17.	Image-17	5.90	0.002202	74.70	0.9699
18.	Image-18	6.01	0.018293	65.50	0.9782
19.	Image-19	6.10	0.000959	78.31	0.9131
20.	Image-20	6.01	0.008873	68.64	0.9845
21.	Image-21	5.80	0.004192	71.90	0.9734
22.	Image-22	6.20	0.005833	70.47	0.9474
23.	Image-23	6.01	0.002400	74.32	0.9518
24.	Image-24	5.70	0.000910	78.53	0.9275
25.	Image-25	6.01	0.002135	74.83	0.9477
26.	Image-26	6.00	0.002729	73.76	0.9692
27.	Image-27	6.30	0.002193	74.71	0.9177
28.	Image-28	6.01	0.000718	79.56	0.9776
29.	Image-29	6.01	0.011136	67.66	0.9295
30.	Image-30	6.00	0.006919	69.72	0.9494
Average		6.00	0.005282	72.60	0.9517

Fig. 10 show the reconstructed images of the ESDCA-DSDCA model. As seen in Table I, we have computed and analyzed the model's performance and the reconstructed image's quality. The ESDCA-DSDCA scheme achieved a more excellent SS (%) value, 3.6262, than the DWT-CNN scheme. Also, The ESDCA-DSDCA scheme achieved a greater PSNR value, 15.078, over the DWT-CNN scheme. We have noticed that the ESDCA-DSDCA scheme achieved the most significant CR, 6.3, for image-19 and the smallest CR value, 5.70, for image-9. We have seen that the ESDCA-DSDCA scheme achieved the most significant MSE value, 0.018293, for image-18 and the smallest MSE value, 0.000718, for image-28.

The ESDCA-DSDCA scheme achieved the most significant

PSNR value, 79.56 dB, for image-28, and the smallest PSNR value, 65.50 dB, for image-18. We have computed and analyzed the model's performance and the reconstructed image's quality. The ESDCA-DSDCA scheme achieved a more excellent SS (%) value, 3.63, than the DWT-CNN scheme. Table II shows that we have computed and analyzed the model's performance and the reconstructed image's quality. Also, The ESDCA-DSDCA scheme achieved a greater PSNR value, 15.77, over the DWT-CNN scheme. We have noticed that the ESDCA-DSDCA scheme achieved the most significant CR, 6.3, for image-12 and the smallest CR value, 5.7, for image-5. We have seen that the ESDCA-DSDCA scheme achieved the most significant MSE value, 0.007385, for image-6 and the smallest MSE value, 0.000647, for image-15. The ESDCA-DSDCA scheme achieved the most significant PSNR value, 80.02 dB, for image-15, and the smallest PSNR value, 69.45 dB, for image-6. The contents of Table II have illustrated the ESDCA-DSDCA model's experimental results. Table III and Table IV have represented and compared the average SS (%) and PSNR of ESDCA-DSDCA, JPEG2000, JPEG, SR-CNN, and DWT-CNN methods. It has been shown that the SS (%) of the ESDCA-DSDCA scheme has been achieved more significantly than the SS (%) of the JPEG2000, JPEG, SR-CNN, and DWT-CNN schemes. Also, Fig. 11 and Fig. 12 have visually shown that the ESDCA-DSDCA model's SS (%) has been higher than the SS (%) of the ESDCA-DSDCA scheme, and the SS (%) of JPEG2000, JPEG, SR-CNN, and DWT-CNN.

TABLE II
EXPERIMENTAL RESULTS OF ESDCA-DSDCA
FOR DATASET: SEA ANIMAL

Sl. No.	Test Images	CR	MSE	PSNR (dB)	SSIM
1.	Image-1	6.01	0.003081	73.24	0.9753
2.	Image-2	5.90	0.002769	73.71	0.9961
3.	Image-3	6.01	0.001694	75.84	0.9951
4.	Image-4	6.10	0.002289	74.53	0.9505
5.	Image-5	5.70	0.003639	72.52	0.9849
6.	Image-6	5.80	0.007385	69.45	0.9899
7.	Image-7	6.20	0.001786	75.61	0.9885
8.	Image-8	6.01	0.005431	70.78	0.9537
9.	Image-9	6.01	0.001407	76.65	0.9626
10.	Image-10	6.01	0.002603	73.98	0.9581
11.	Image-11	6.00	0.000952	78.35	0.9406
12.	Image-12	6.30	0.001093	77.75	0.9886
13.	Image-13	6.01	0.002543	74.08	0.9943
14.	Image-14	6.01	0.001915	75.31	0.9934
15.	Image-15	6.00	0.000647	80.02	0.9686
16.	Image-16	5.81	0.002946	73.44	0.9962
17.	Image-17	6.01	0.002473	74.19	0.9716
18.	Image-18	6.00	0.000994	78.16	0.9654
19.	Image-19	6.30	0.002336	74.45	0.9639
20.	Image-20	6.01	0.002814	73.64	0.9935
21.	Image-21	6.00	0.001906	75.33	0.9652
22.	Image-22	6.01	0.001288	77.03	0.9938
23.	Image-23	5.90	0.003428	72.78	0.9759
24.	Image-24	6.01	0.001269	77.09	0.9813
25.	Image-25	6.01	0.005019	71.13	0.9757
26.	Image-26	6.00	0.003181	73.11	0.9782
27.	Image-27	5.90	0.003041	73.30	0.9782
28.	Image-28	6.01	0.002898	73.51	0.9694
29.	Image-29	6.00	0.002489	74.17	0.9681
30.	Image-30	6.10	0.000662	79.92	0.9817
Average		6.00	0.002533	74.77	0.9766

TABLE III
COMPARATIVE VALUES OF PSNR, SSIM AND SS(%)
FOR DATA SET: MARINE ANIMALS

Sl. No.	Methods	SS (%)	PSNR (dB)	SSIM
1.	JPEG2000 [2]	70.12	50.96	0.9275
2.	JPEG [2], [15]	74.43	48.01	0.9131
3.	SR-CNN [2]	76.43	52.80	0.9368
4.	DWT-CNN [2], [32]	79.7038	57.52	0.9403
5.	Proposed	83.33%	72.60	0.9517

TABLE IV
COMPARATIVE VALUES OF PSNR, SSIM AND SS(%)
FOR DATASET: SEA ANIMAL

Sl. No.	Methods	SS (%)	PSNR (dB)	SSIM
1.	JPEG2000 [2]	70.12	52.32	0.9275
2.	JPEG [2], [15]	74.43	48.44	0.9131
3.	SR-CNN [2]	76.43	54.18	0.9368
4.	DWT-CNN [2], [32]	79.7038	58.99	0.9403
5.	Proposed	83.33%	74.77	0.9766

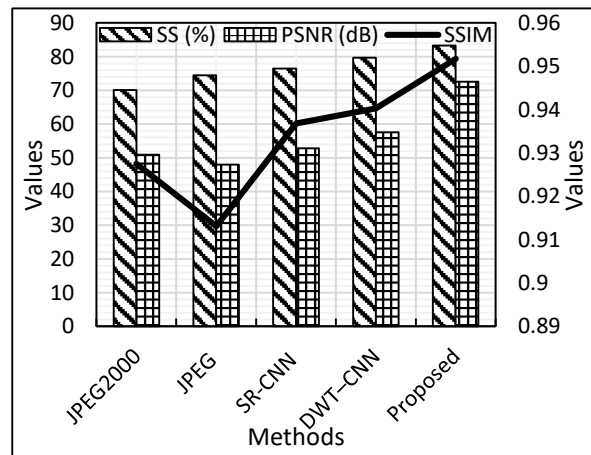


Fig. 11. Graphical Interpretation of Experimental Results of five different Methods: Dataset: Marin Animals

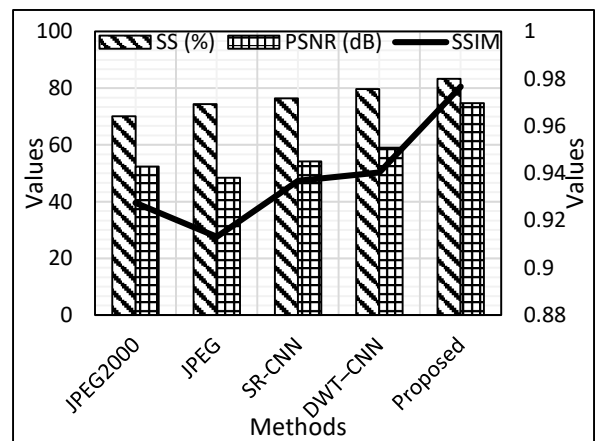


Fig. 12. Graphical Interpretation of Experimental Results of five different Methods: Dataset: Sea Animal

The figure shows the average SS (%) to quickly understand the SS (%) of JPEG2000, JPEG, SR-CNN, and DWT-CNN models. So, we have noticed that the proposed image compression scheme provided a more significant SS value of 83.33% and SSIM value 0.9766 than the JPEG2000, JPEG,

SR-CNN, and DWT-CNN models. Finally, the proposed image compression scheme ESDCA-DSDCA is a valuable image compression model.

V. CONCLUSION

The everyday use of IoT applications is growing, and transmitting multimedia data necessitates implementing an effective image compression model, mainly for aquatic circumstances. In this article, we have developed an image compression method based on ESDCA and DSDCA. We have described an effective learning technique that uses ESDCA and DSDCA to represent the image compactly and effectively. The ESDCA-DSDCA model is also highly suitable, like available standards image compression methods, JPEG2000, JPEG, SR-CNN, and DWT-CNN. The outcomes show the superiority of the ESDCA-DSDCA models over the state-of-the-art models for the performance measures. The ESDCA-DSDCA method efficiently indicates the trade-off between the CR and PSNR, giving a higher SS(%) value of 83.33, a PSNR value of 72.60 (dB), and SSIM value of 0.9517 for the Marine Animals dataset. Also, the proposed model achieved SS(%) value of 83.33, PSNR of 74.77 (dB), and SSIM of 0.9766 values for the Sea Animal dataset. The ESDCA-DSDCA model will investigate the outcome in noisy environments, and the denoising procedure will enhance the results. The model works very well, given that for only 25 epochs, the model performs well. Its compression accuracy will increase by increasing the significant number of datasets to train and test the model. If the model trains for a large dataset, it will perform better.

REFERENCES

- [1] Fei Yuan, Lihui Zhan, Panwang Pan, and En Cheng, "Low bit-rate compression of underwater image based on human visual system," *Signal Processing: Image Communication*, vol. 91, pp. 1-15, 2021.
- [2] N. Krishnaraj, Mohamed Elhoseny, M. Thenmozhi, Mahmoud M. Selim, and K. Shankar, "Deep learning model for real-time image compression in Internet of Underwater Things (IoUT)," *Journal of Real-Time Image Processing*, vol. 17, pp. 2097-2111, 2020.
- [3] Ian Goodfellow, Jean Pouget-Abadie, Mehdi Mirza, Bing Xu, David Warde-Farley, Sherjil Ozair, Aaron Courville, and Yoshua Bengio, "Generative adversarial networks," *Communications of the ACM*, vol. 63, no. 11, pp. 139-144, 2020.
- [4] Feng Jiang, Wen Tao, Shaohui Liu, Jie Ren, Xun Guo, and Debin Zhao, "An end-to-end compression framework based on convolutional neural networks," *IEEE Transactions on Circuits and Systems for Video Technology*, vol. 28, no. 10, pp. 3007-3018, 2017.
- [5] John Y. Chiang, and Ying-Ching Chen, "Underwater image enhancement by wavelength compensation and dehazing," *IEEE transactions on image processing*, vol. 21, no. 4, pp. 1756-1769, 2012.
- [6] Pierre Baldi, "Auto-encoders, unsupervised learning, and deep architectures," In *Proceedings of ICML workshop on unsupervised and transfer learning*, JMLR Workshop and Conference Proceedings, 2012, pp. 37-49.
- [7] Forest Agostinelli, Michael R. Anderson, and Honglak Lee, "Adaptive multi-column deep neural networks with application to robust image denoising," *Advances in neural information processing systems*, vol. 26, 2013.
- [8] Johannes Ballé, Valero Laparra, and Eero P. Simoncelli, "End-to-end optimized image compression," *arXiv preprint arXiv:1611.01704*, 2016.
- [9] J. Ballé, V. Laparra, and E. P. Simoncelli, "End-to-end optimized image compression," *5th International Conference on Learning Representations, ICLR Proceedings 2017*, pp.1-9.
- [10] D. Alexandre, C. P. Chang, W. H. Peng, and H. M. Hang, "An autoencoder-based learned image compressor: Description of challenge proposal by NCTU," In *Proceedings of the IEEE Conference on Computer Vision and Pattern Recognition Workshops 2018*, pp. 2539-2542.
- [11] L. Cavigelli, P. Hager, and L. Benini, "CAS-CNN: A deep convolutional neural network for image compression artifact suppression," In *2017 International Joint Conference on Neural Networks (IJCNN) IEEE*, 2017, pp. 752-759.
- [12] Z. Cheng, H. Sun, M. Takeuchi, and J. Katto, "Deep convolutional autoencoder-based lossy image compression," In *2018 Picture Coding Symposium (PCS) IEEE*, 2018, pp. 253-257.
- [13] Lucas Theis, Wenzhe Shi, Andrew Cunningham, and Ferenc Huszár, "Lossy image compression with compressive autoencoders," *arXiv preprint arXiv:1703.00395*, 2017.
- [14] T. G. Shirsat and V. K. Bairagi, "Lossless medical image compression by integer wavelet and predictive coding," *International Scholarly Research Notices* 2013, pp. 1-6.
- [15] G. Toderici, D. Vincent, N. Johnston, S. J. Hwang, D. Minnen, J. Shor, and M. Covell, "Full resolution image compression with recurrent neural networks," In *Proceedings of the IEEE conference on Computer Vision and Pattern Recognition*, 2017, pp. 5306-5314.
- [16] J. Jiang, "Image compression with neural networks—a survey," *Signal processing: image Communication*, vol. 14, no. 9, pp. 737-760, 1999.
- [17] Sea animals image dataset available online: <https://www.kaggle.com/datasets/vencerlanz09/sea-animals-image-dataset> (accessed on 19 Nov, 2022)
- [18] Shibani Santurkar, David Budden, and Nir Shavit, "Generative compression," In *2018 Picture Coding Symposium (PCS), IEEE*, 2018, pp. 258-262.
- [19] R. C. Woods, "Digital Image processing," New Delhi: 3rd ed, Low price edition, Pearson Pentice Hall, 2008, pp. 1-904.
- [20] R. C. Gonzalez and R. E. Woods, "Digital Image Processing," 3rd ed., India, Pearson, 2008, pp. 1-976.
- [21] K. Sayood, "Introduction to Data Compression," 3rd ed., USA, M.K. is an imprint of Elsevier, 2006, pp. 1-566.
- [22] Underwater Image Datasets available online: <https://www.kaggle.com/datasets/Underwater Image> (accessed on 26 Sept, 2022)
- [23] Raimondo Schettini, and Corchs Silvia, "Underwater image processing: state of the art of restoration and image enhancement methods," *EURASIP journal on advances in signal processing* 2010, pp. 1-14, 2010.
- [24] A. Y. Tolstonogov, and A. D. Shiryayev, "The Image Semantic Compression Method for Underwater Robotic Applications," In *OCEANS 2021: San Diego-Porto*, IEEE, 2021, pp. 1-9.
- [25] Ya-qiong Cai, Hai-xia Zou, and Fei Yuan, "Adaptive compression method for underwater images based on perceived quality estimation," *Frontiers of Information Technology & Electronic Engineering* vol. 20, no. 5, pp. 716-730, 2019.
- [26] Y. Wang, J. Zhang, Y. Cao, and Z. Wang, "A deep CNN method for underwater image enhancement," In *2017 IEEE international conference on image processing (ICIP)*, IEEE, 2017, pp. 1382-1386.
- [27] Anushka Yadav, Mayank Upadhyay, and Ghanapriya Singh, "Underwater Image Enhancement Using Convolutional Neural Network," *arXiv preprint arXiv:2109.08916*, 2021.
- [28] Yudong Wang, Jichang Guo, Huan Gao, and Huihui Yue, "UIEC²-Net: CNN-based underwater image enhancement using two color space," *Signal Processing: Image Communication* vol. 96, 116250, 2021.
- [29] Y. Wang, J. Zhang, Y. Cao, and Z. Wang, "A deep CNN method for underwater image enhancement," In *2017 IEEE international conference on image processing (ICIP)*, IEEE, 2017, pp. 1382-1386.
- [30] Fenglei Han, Jingzheng Yao, Haitao Zhu, and Chunhui Wang, "Underwater image processing and object detection based on deep CNN method," *Journal of Sensors*, 2020.
- [31] Azim Akhtarshenas, and Ramin Toosi, "An open-set framework for underwater image classification using autoencoders," *SN Applied Sciences*, vol. 4, no. 8, p. 229, 2022.
- [32] Raj Kumar Paul, and Saravanan Chandran. "A Health Care Image Compression Scheme using Discrete Wavelet Transform and Convolution Neural Network." *Journal of Engineering Research*, vol. 10, pp. 1-15, 2022.
- [33] R. K. Paul, and S. Chandran. "Image Compression Using Histogram Equalization." In *Innovations in Computational Intelligence and Computer Vision: Proceedings of ICICV 2021*, Singapore: Springer Nature Singapore, 2022, pp. 47-61.
- [34] R. K. Paul, and S. Chandran. "Image Compression Scheme Based on Histogram Equalization and Convolution Neural Network." In *Data Engineering and Intelligent Computing: Proceedings of 5th ICICC 2021*, Singapore: Springer Nature Singapore, 2022, vol. 1, pp. 327-340.
- [35] Chi-Hung Chuang, Cheng-Tan Tung, Yuan-Song Chang, Edward Lin, Chih-Ping Yen, "Facial Feature Classification of Drug Addicts Using Deep Learning," *Engineering Letters*, vol. 31, no.3, pp1096-1103, 2023

- [36] Yu Wang, Changfeng Zhu, Qingrong Wang, and Jinhao Fang, "Research on Fault Detection of Rolling Bearing Based on CWT-DCCNN-LSTM," *Engineering Letters*, vol. 31, no.3, pp987-1000, 2023
- [37] Anita Desiani, Erwin, Bambang Suprihatin, Ermatita, Fathur R. Husein, and Yogi Wahyudi, "A Novelty Patching of Circular Random and Ordered Techniques on Retinal Image to Improve CNN U-Net Performance," *Engineering Letters*, vol. 30, no.4, pp1217-1229, 2022

Raj Kumar Paul (M'40), born at Nedhua (Sabang, Paschim Medinipur, West Bengal, India) on 05 Jan 1983. He is pursuing Ph.D. in Computer Science and Engineering at the National Institute of Technology Durgapur, West Bengal, India. He completed his M.Tech. in Computer Science and Engineering from SRM University, Chennai, Tamil Nadu, India, in July 2009. His primary field of study is Digital Image Processing using traditional methods and the machine learning approach.



He has seven years of research experience (as a Research Project Assistant and Research Fellow) and ten years of teaching experience (as an Assistant Professor). Currently, he is working as an assistant professor at Budge Budge Institute of Technology, Kolkata, West Bengal, India. He published many articles in renowned Journals (Scopus, SCI). His article was recently accepted in the SCI Journal (*Multimedia Tools and Application*) on Oct 9, 2023. Also, his book was accepted as entitled "Advanced Image Processing Systems".

Prof. Paul has many memberships in professional societies. He has a lifetime membership with the Indian Society for Technical Education (ISTE) in Delhi, India. He is an Associate Member of the Institute of Engineers India (IEI), Kolkata, India. Also, he has a membership with Vijnana Bharati (VIBHA), India.

Ankit Vishwakarma is a graduate student of National Institute of Technology, Durgapur, India.

Dr. Saravanan Chandran is an Associate Professor of National Institute of Technology, Durgapur, India.